medRxiv preprint doi: https://doi.org/10.1101/2020.06.17.20133892; this version posted June 19, 2020. The copyright holder for this preprint (which was not certified by peer review) is the author/funder, who has granted medRxiv a license to display the preprint in perpetuity. It is made available under a CC-BY-NC-ND 4.0 International license .

Routine laboratory blood tests predict SARS-CoV-2 infection using machine learning

He Sarina Yang[1,2*], Ljiljana V. Vasovic[1,3], Peter Steel[1,4], Amy Chadburn[1,2], Yu Hou[5], Sabrina E. Racine-Brzostek[1,2], Melissa M. Cushing[1,2], Massimo Loda[1,2], Rainu Kaushal[2,5], Zhen Zhao[1,2*], Fei Wang[5*]

[1]Department of Pathology and Laboratory Medicine, Weill Cornell Medicine, New York, NY, USA

[2] New York-Presbyterian Hospital, Weill Cornell Medicine, New York, NY, US

[3] New York-Presbyterian Hospital, Lower Manhattan Hospital, New York, NY, US

[4]Department of Emergency Medicine, Weill Cornell Medicine, New York, NY, USA

[5]Department of Population Health Sciences, Weill Cornell Medicine, New York, NY, USA

*Joint corresponding authors.

Correspondence to:

Fei Wang, PhD

Division of Health Informatics

Department of Healthcare Policy and Research

NOTE: This preprint reports new research that has not been certified by peer review and should not be used to guide clinical practice.

medRxiv preprint doi: https://doi.org/10.1101/2020.06.17.20133892; this version posted June 19, 2020. The copyright holder for this preprint (which was not certified by peer review) is the author/funder, who has granted medRxiv a license to display the preprint in perpetuity. It is made available under a CC-BY-NC-ND 4.0 International license .

Weill Cornell Medicine

425 E. 61th Street, New York City, NY 10065

Email: few2001@med.cornell.edu

Phone: 646-962-9405

Zhen Zhao, PhD

Department of Pathology and Laboratory Medicine

Weill Cornell Medicine

525 E. 68th Street, Suite F 701, New York, NY 10065

Email: zhz9010@med.cornell.edu

Phone: 212-746-2682

He S. Yang, PhD

Department of Pathology and Laboratory Medicine

Weill Cornell Medicine

525 E. 68th Street, Suite F 701, New York, NY 10065

Email: hey9012@med.cornell.edu

Phone: 212-746-6292

medRxiv preprint doi: https://doi.org/10.1101/2020.06.17.20133892; this version posted June 19, 2020. The copyright holder for this preprint (which was not certified by peer review) is the author/funder, who has granted medRxiv a license to display the preprint in perpetuity. It is made available under a CC-BY-NC-ND 4.0 International license .

Running title: Routine laboratory tests predict SARS-CoV-2 infection

Key words: SARS-CoV-2, COVID-19, machine learning, gradient boosted decision tree, routine laboratory tests

Abstract word count: 250; Word count of manuscript text: 2930

Abbreviation: COVID-19: corona virus disease-2019; SARS-CoV-2: severe acute respiratory syndrome coronavirus 2; TAT: turn-around time; ED: emergency department; ICU: intensive care unit; RT-PCR: real-time reverse transcription polymerase chain reaction; GBDT: gradient boosted decision tree; HCP: healthcare personnel; WBC: white blood cells; RBC: red blood cells; LDH: lactic acid dehydrogenase; RDW-CV: Red blood cell distribution width; ALT: Alanine aminotransferase; AST: Aspartate aminotransferase; ALK: Alkaline phosphatase; BUN: Blood urea nitrogen; MCH: Mean corpuscular hemoglobin; MCV: Mean corpuscular volume; aPTT: Activated partial thromboplastin time; CRP: C-reactive protein; INR: International normalized ratio; PT: Prothrombin time;

medRxiv preprint doi: https://doi.org/10.1101/2020.06.17.20133892; this version posted June 19, 2020. The copyright holder for this preprint (which was not certified by peer review) is the author/funder, who has granted medRxiv a license to display the preprint in perpetuity. It is made available under a CC-BY-NC-ND 4.0 International license .

Abstract:

Background: Accurate diagnostic strategies to rapidly identify SARS-CoV-2 positive individuals for management of patient care and protection of health care personnel are urgently needed. The predominant diagnostic test is viral RNA detection by RT-PCR from nasopharyngeal swabs specimens, however the results of this test are not promptly obtainable in all patient care locations. Routine laboratory testing, in contrast, is readily available with a turn-around time (TAT) usually within 1-2 hours.

Method: We developed a machine learning model incorporating patient demographic features (age, sex, race) with 27 routine laboratory tests to predict an individual's SARS-CoV-2 infection status. Laboratory test results obtained within two days before the release of SARS-CoV-2-RT-PCR result were used to train a gradient boosted decision tree (GBDT) model from 3,346 SARS-CoV-2 RT-PCR tested patients (1,394 positive and 1,952 negative) evaluated at a large metropolitan hospital.

Results: The model achieved an area under the receiver operating characteristic curve (AUC) of 0.853 (95% CI: 0.829-0.878). Application of this model to an independent patient dataset from a separate hospital resulted in a comparable AUC (0.838), validating the generalization of its use. Moreover, our model predicted initial SARS-CoV-2 RT-PCR positivity in 66% individuals whose RT-PCR result changed from negative to positive within two days.

Conclusion: This model employing routine laboratory test results offers opportunities for early and rapid identification of high-risk SARS-COV-2 infected patients before their RT-PCR results are available. This may facilitate patient care and quarantine, indicate

medRxiv preprint doi: https://doi.org/10.1101/2020.06.17.20133892; this version posted June 19, 2020. The copyright holder for this preprint (which was not certified by peer review) is the author/funder, who has granted medRxiv a license to display the preprint in perpetuity. It is made available under a CC-BY-NC-ND 4.0 International license .

who requires retesting, and direct personal protective equipment use while awaiting definitive RT-PCR results.

medRxiv preprint doi: https://doi.org/10.1101/2020.06.17.20133892; this version posted June 19, 2020. The copyright holder for this preprint (which was not certified by peer review) is the author/funder, who has granted medRxiv a license to display the preprint in perpetuity. It is made available under a CC-BY-NC-ND 4.0 International license .

Introduction:

The Coronavirus Disease-2019 (COVID-19) pandemic has rapidly spread worldwide resulting in over 7 million confirmed cases and more than 368,000 total deaths as of June 9, 2020 *(1)*. The highly contagious nature of SARS-CoV-2 *(2),* rapid progression of disease in some infected patients *(3)* and the subsequent stress on the healthcare system has created an urgent need for rapid and effective diagnostic strategies for the prompt identification and isolation of infected patients. Currently, the diagnosis of COVID-19 relies on SARS-CoV-2 virus-specific real-time reverse-transcriptase polymerase chain reaction (RT-PCR) testing of nasopharyngeal swabs or other upper respiratory track specimens *(4, 5)*. However, while the TAT of RT-PCR testing is usually within 48 hours *(6)*, it can be significantly longer due to many variables including the need for repeat testing or the lack of needed supplies. Many emergency departments (EDs) in smaller hospitals do not yet have access to on-site SARS-CoV-2 RT-PCR testing. These issues can result in delayed hospital admission and bed assignment, inappropriate medical management including quarantining of infected patients and increased exposure of healthcare personnel and other patient contacts to the virus. Rapid diagnosis and identification of high risk patients for early intervention is vital for individual patient care, and, from a public health perspective, for controlling disease transmission and maintaining the healthcare workforce.

Currently in hospital EDs, the nationally recommended practice when evaluating patients with moderate to high risk for COVID-19 is SARS-CoV-2 RT-PCR testing, a panel of routine laboratory tests, a chest X-ray and symptomatology, whereas chest computed tomography (CT) is not recommended due to cost and TAT considerations

medRxiv preprint doi: https://doi.org/10.1101/2020.06.17.20133892; this version posted June 19, 2020. The copyright holder for this preprint (which was not certified by peer review) is the author/funder, who has granted medRxiv a license to display the preprint in perpetuity. It is made available under a CC-BY-NC-ND 4.0 International license .

(2, 7). Routine laboratory tests are generally available within 1-2 hours and are accessible prior to patient discharge from the ED. Several studies *(3, 8-10)* have reported laboratory abnormalities in COVID-19 patients on admission and during the disease course, including elevations of C-reactive protein (CRP), D-dimer, lactic acid dehydrogenase (LDH), cardiac troponin, procalcitonin (PCT), and creatinine as well as lymphopenia, thrombocytopenia, leukopenia. While no single laboratory test can accurately discriminate SARS-CoV-2 infected from non-infected patients, the combination of the results of these routine laboratory tests may predict the COVID-19 status.

Recent promising advances in the application of artificial intelligence (AI) in several healthcare areas *(11-13)* have inspired the development of AI-based algorithms as diagnostic *(14)* or prognosis tools *(15)* for complex diseases, such as COVID-19. In this study, we hypothesized that the results of routine laboratory tests performed within a short time frame as the RT-PCR testing, in conjunction with a limited number of previously identified predictive demographic factors (age, gender, race) *(16)*, can predict SARS-CoV-2 infection status. Thus, we aimed to develop a machine learning model integrating age, gender, race and routine laboratory blood tests, which are readily available with a short TAT.

medRxiv preprint doi: https://doi.org/10.1101/2020.06.17.20133892; this version posted June 19, 2020. The copyright holder for this preprint (which was not certified by peer review) is the author/funder, who has granted medRxiv a license to display the preprint in perpetuity. It is made available under a CC-BY-NC-ND 4.0 International license .

Methods

Data collection:

We conducted a retrospective study with 5,893 patients evaluated at the New York Presbyterian Hospital/Weill Cornell Medicine (NYPH/WCM) during March 11 to April 29, 2020. SARS-CoV-2 RT-PCR results, routine laboratory testing results and patient demographic information were obtained from electronic medical records (EMR, Allscripts, Chicago, IL). Exclusion criteria included patients < 18 years, patients who had indeterminate RT-PCR results, and patients who did not have any laboratory results within two days prior to the completion of RT-PCR testing. Data from 1,394 RT-PCR positive and 1,952 negative patients were used in our analysis. Same criteria were applied to the dataset collected from New York Presbyterian Hospital/Lower Manhattan Hospital (NYPH/LMH) during the same time period. Data from 549 RT-PCR positive and 1,273 negative LYPH/LMH patients were obtained and used for validation. This study was approved by the Institutional Review Board (#20-03021671) of Weill Cornell Medicine.

SARS-CoV-2 RT-PCR testing

SARS-CoV-2 RT-PCR testing was performed using the RealStar SARS-CoV-2 RT-PCR kit 1.0 (Altona Diagnostics) reagent system, the Cobas SARS-CoV-2 RT-PCR assay (Roche Diagnostics), the Panther Fusion SARS-CoV-2 RT-PCR assay (Hologic), and Xpert Xpress SARS-CoV-2 RT-PCR (Cepheid) at NYPH/WCM. RT-PCR was performed using the Xpert Xpress SARS-CoV-2 RT-PCR (Cepheid) at NYPH/LMH.

medRxiv preprint doi: https://doi.org/10.1101/2020.06.17.20133892; this version posted June 19, 2020. The copyright holder for this preprint (which was not certified by peer review) is the author/funder, who has granted medRxiv a license to display the preprint in perpetuity. It is made available under a CC-BY-NC-ND 4.0 International license .

Nucleic acid from patient nasopharyngeal (NP) swab samples and added control RNA were simultaneously extracted. Real-time RT-PCR technology utilizes reverse-transcriptase (RT) to convert RNA into complementary DNA (cDNA), polymerase chain reaction (PCR) to amplify specific target sequences, and specific probes to detect the amplified DNA.

Routine Laboratory testing:

At WCM, routine chemistry testing was performed on Siemens ADVIA XPT analyzers and Centaur XP analyzers (Erlangen, Germany). Procalcitonin was performed on Roche e411 analyzer (Basel, Switzerland). Blood gas analysis was performed on Instrumentation Laboratory GEM Premier 4000 analyzer (Bedford, MA, USA). Routine hematological testing was performed on the UniCel DXH 800 analyzer (Nyon, Switzerland). Coagulation tests was performed on Instrumentation Laboratory ACLTM TOP CTS Coagulation System.

At LMH, Routine chemistry testing including procalcitonin were performed on ABBOTT® ARCHITECT c SYSTEM ci 4100 and ci 8200 analyzers (Chicago, IL, USA). Blood gas analysis was performed on Radiometer analyzer ABL 820 FLEX (Copenhagen, Denmark). Routine complete blood count (CBC) testing was performed on the UniCel DXH 800 analyzer. Coagulation tests were performed on STAGO STA-R® Evolution multiparametric analyzer (Parsippany, New Jersey, USA).

Model construction:

medRxiv preprint doi: https://doi.org/10.1101/2020.06.17.20133892; this version posted June 19, 2020. The copyright holder for this preprint (which was not certified by peer review) is the author/funder, who has granted medRxiv a license to display the preprint in perpetuity. It is made available under a CC-BY-NC-ND 4.0 International license .

A total of 685 distinct laboratory tests were ordered for patients in the WCM dataset. A 685-dimensional vector was generated for each RT-PCR test. If one specific test was ordered multiple times, an average of the values was calculated and used for analysis. Univariate analysis was performed on all laboratory test results to obtain the significance of the association between each laboratory test and the RT-PCR result. For laboratory tests with continuous values, we applied the Mann-Whitney U test using the scipy.stats.mannwhitneyu function in SciPy 1.4.1 (https://scipy.org/). For laboratory tests with nominal values, we applied the chi-square test using scipy.stats.chisquare in SciPy 1.4.1. The Fisher's exact test was performed if the number was too small (<5) for certain values of the laboratory test using the fisher.test function in R. Laboratory tests were selected to construct the input feature vectors of the prediction model based on the following criteria: 1) a result available for at least 30% of the patients two days before a specific SARS-CoV-2 RT-PCR test, and 2) showing a significant difference (p-value, p-value after Bonferroni correction, p-value after demographics adjustment all less than 0.05) between patients with positive and negative RT-PCR results. Laboratory tests having redundant clinical information were eliminated. For example, for neutrophil count and percentage, only the absolute neutrophil count was retained for analysis. After this procedure, twenty-seven routine laboratory tests were selected for further analysis.

A 33-dimensional vector (27 routine lab tests, 1 age, 1 gender, 4 race variables corresponding to White, Black, Asian and others) was constructed to represent every RT-PCR test. The value on each dimension was the average result value of the corresponding laboratory test taken two days before the RT-PCR test in addition to the patients' age, gender and race. The patient's race and gender variables were encoded

medRxiv preprint doi: https://doi.org/10.1101/2020.06.17.20133892; this version posted June 19, 2020. The copyright holder for this preprint (which was not certified by peer review) is the author/funder, who has granted medRxiv a license to display the preprint in perpetuity. It is made available under a CC-BY-NC-ND 4.0 International license .

with binary values. The missing value of a specific laboratory test in a feature vector was imputed by the median value of the available non-missing value of that dimension over all patients. The result of each RT-PCR test was referred to as the label of the test.

Mathematically, let $\boldsymbol{x}_i$ be the 33-dimensional feature vector of the i-th RT-PCR test. Let $y_i \in \{0,1\}$ be its corresponding label. $y_i = 0$ means the result of the i-th RT-PCR test is "Not Detected" and we refer to this RT-PCR test as a negative sample, while $y_i = 1$ means the result is "Detected" and we refer to this RT-PCR test as a positive sample. Our goal was to "learn" a classification function f that can accurately map each $\boldsymbol{x}_i$ to its corresponding y_i. We considered 4 popular classifiers in this study:

- Logistic regression, where f is a linear function and our implementation is based on the scikit-learn package 0.23.1 using sklearn.linear_model.LogisticRegression with all default parameter settings
- Decision tree, where f is a classification tree and our implementation is based on the scikit-learn package 0.23.1 with sklearn.tree.DecisionTreeClassifier with all default parameter settings. According to the document (https://scikit-learn.org/stable/modules/tree.html#tree-algorithms-id3-c4-5-c5-0-and-cart), the decision tree algorithm implemented in scikit-learn is an optimized Classification and Regression Tree (CART) algorithm *(17)*.
- Random forest, where f is a random forest*(18)* and our implementation is based on scikit-learn package 0.23.1 with sklearn.ensemble.RandomForestClassifier with all default parameter settings and the number of trees equal 100.
- Gradient boosted decision tree (GBDT), where f is a gradient boosting machine with decision tree as base learners *(19)*. Our implementation is based on scikit-

medRxiv preprint doi: https://doi.org/10.1101/2020.06.17.20133892; this version posted June 19, 2020. The copyright holder for this preprint (which was not certified by peer review) is the author/funder, who has granted medRxiv a license to display the preprint in perpetuity. It is made available under a CC-BY-NC-ND 4.0 International license .

learn package 0.23.1 with sklearn.ensemble.GradientBoostingClassifier with all default parameter settings and the number of trees equal 100.

The models were evaluated in two different settings. The first setting was a 5-fold cross validation with the NYPH/WCM data, where all RT-PCR tests were randomly partitioned into 5 equal buckets with the same positive/negative ratio in each bucket as the ratio over all tests. The implementation was based on scikit-learn package 0.23.1 with the sklearn.model_selection.StratifiedKFold function. Then the training and testing procedure was performed 5 times for these 4 different classifiers. Each time a specific bucket (fold) was used for testing and the remaining 4 buckets (folds) for training. In the second setting all data from NYPH/WCM were used for training, and the data from LMH was used for testing. In both settings, highly suspicious negatives (HSN) were excluded in the training process. Here an HSN was defined as a negative RT-PCR test in a patient who had a positive RT-PCR result upon re-testing within 2 days.

medRxiv preprint doi: https://doi.org/10.1101/2020.06.17.20133892; this version posted June 19, 2020. The copyright holder for this preprint (which was not certified by peer review) is the author/funder, who has granted medRxiv a license to display the preprint in perpetuity. It is made available under a CC-BY-NC-ND 4.0 International license .

Results:

The pipeline of our modeling framework is illustrated in Figure 1. A summary of statistics of the 27 routine laboratory tests used to construct the input feature vectors of the prediction model is shown in Table 1. The models were trained and tested on a retrospective dataset collected from 3,346 SARS-CoV-2 RT-PCR tested adult patients who had routine laboratory testing performed within two days prior to the release of RT-PCR result, between March 11 to April 29, 2020, at NYPH/WCM. This dataset included 1,394 SARS-CoV-2 RT-PCR positive and 1,952 negative patients who ranged in age from 18 to 101 years (mean 56.4 years, demographic information in Table 2). Among 590 patients who had repeat testing during this 7-week study period, 53 were initially negative but became positive upon repeat testing. Among this subgroup, 60% (32 out of 53) patients' RT-PCR results changed from negative to positive within a 2-day period.

The performance of four machine learning models from 5-fold cross validation are summarized in Figure 2. The GBDT model achieved the best performance with an area under the receiver operating characteristic curve (AUC) value of 0.853 (95% CI: 0.829 - 0.878), sensitivity of 0.758 (95% CI: 0.662 - 0.812) and specificity of 0.802 (95% CI: 0.767 – 0.909) at the operating point determined by the maximum Youden Index *(20)*. As an independent validation, we tested the performance of the trained model on an independent patient dataset (549 positive and 1,273 negative by RT-PCR, Table 2) collected from NYPH/LMH] during the same time period as the WCM site. Using the model trained on NYP/WCM patients, we are able to obtain an AUC of 0.838 on the LMH data, confirming the ability to generalize our model to other hospitals. Given the same sensitivity (0.758) as WCM, the specificity reached 0.740.

medRxiv preprint doi: https://doi.org/10.1101/2020.06.17.20133892; this version posted June 19, 2020. The copyright holder for this preprint (which was not certified by peer review) is the author/funder, who has granted medRxiv a license to display the preprint in perpetuity. It is made available under a CC-BY-NC-ND 4.0 International license .

To further interpret the trained GBDT model, we adopted the Shapley additive explanations (SHAP)*(21)* technique using the SHAP package (https://github.com/slundberg/shap). It assigns each feature an importance value (the Shapley value) for each specific classification. The summary plot of the impact of laboratory tests to the final prediction is shown in Figure 3a. For instance, larger values of lactic acid dehydrogenase (LDH) drive a positive prediction, whereas smaller values of lymphocyte count drive a negative prediction. In addition, lower values of troponin were seen in COVID-19 positive patients than the control group, who were also ill patients coming to hospital for other causes, such as myocardial infarction.

Among the 32 patients whose SARS-CoV-2 RT-PCR results were initially negative but upon repeat testing within two days were positive, our approach predicted positive a result of the initial RT-PCR for 21 patients (66%). For example, a Hispanic male patient in his 70s underwent a RT-PCR testing which showed a negative result. Since the second RT-PCR test taken on the next day was positive, the initial RT-PCR was a suspicious false negative result possibly due to improper sample collection technique. The SHAP force plot (Figure 3c) illustrates how routine laboratory test results and demographics act as “forces” to push the GBDT model to make positive or negative predictions. The significant elevation of LDH, CRP, and ferritin in addition to lymphopenia and hypocalcemia in this patient, as well as his age, all contributed to a positive prediction by the GBDT model (positive probability = 0.95, 0.35 cutoff by the Youden Index), matching the subsequent RT-PCR result. Thus, our model may identify individuals with initial negative SARS-CoV-2 RT-PCR who should be retested and who

medRxiv preprint doi: https://doi.org/10.1101/2020.06.17.20133892; this version posted June 19, 2020. The copyright holder for this preprint (which was not certified by peer review) is the author/funder, who has granted medRxiv a license to display the preprint in perpetuity. It is made available under a CC-BY-NC-ND 4.0 International license .

could potentially need isolation at home or in the hospital while awaiting confirmatory RT-PCR results.

We also varied the length of the window for collecting routine lab tests with 4 more settings: one day before RT-PCR, one day after RT-PCR, one day before and one day after RT-PCR, two days before and one day after RT-PCR. The ROC curves are plotted as Supplemental Figure 2. With this analysis we observed that the longer the time window around the RT-PCR test, with more information captured characterizing patient infection status, resulted in slightly higher prediction performance in terms of AUC. However, these performances did not significantly differ from each other or from the chosen setting.

medRxiv preprint doi: https://doi.org/10.1101/2020.06.17.20133892; this version posted June 19, 2020. The copyright holder for this preprint (which was not certified by peer review) is the author/funder, who has granted medRxiv a license to display the preprint in perpetuity. It is made available under a CC-BY-NC-ND 4.0 International license .

Discussion:

In this study, we proposed a machine learning model incorporating routine laboratory blood tests and a limited number of demographic features to predict an individual's SARS-CoV-2 infection status. Our model is able to generate a probability score of SARS-CoV-2 infection in real time before RT-PCR results are available, identify the patients with a high risk of being SARS-CoV-2 positive and allow for quicker, more disease specific, patient management. As such, this model could be deployed clinically as an application integrated into the Electronic Medical Record (EMR) system. Using this application, clinicians could be alerted promptly of the infection risk level, allowing for rapid triaging and quarantining of high-risk patients.

A recent study*(6)* proposed a machine learning model integrating chest CT findings with clinical symptoms, exposure history, leukocyte counts, age and sex to assist in the diagnosis of SARS-CoV-2 infection in a Chinese patient cohort. This model could be useful when CT scans are available for all patients. However, CT scans are not recommended as part of the initial routine clinical workup of COVID-19 by the American College of Emergency Physicians (ACEP) *(7)*. In contrast, our model is designed to complement the existing COVID-19 evaluation pathway based on the ACEP COVID-19 Field Guideline *(7)*. Predicting the probability of SARS-CoV-2 infection based on routine laboratory testing *without* radiology evidence is fast and inexpensive. However, it can be challenging because 1) the differences of individual laboratory test results are subtle between infected and non-infected patients at an early stage of the disease; and 2) in practice, patients may not undergo extensive laboratory testing, resulting in missing values in the dataset. In spite of these complications, our model has

medRxiv preprint doi: https://doi.org/10.1101/2020.06.17.20133892; this version posted June 19, 2020. The copyright holder for this preprint (which was not certified by peer review) is the author/funder, who has granted medRxiv a license to display the preprint in perpetuity. It is made available under a CC-BY-NC-ND 4.0 International license .

demonstrated a robust performance and delivers accurate predictions. More importantly, we have proven that the model can be generalized to other hospitals, other patient populations and other laboratory testing environments based on the predictability seen using an independent patient dataset.

The GBDT model was trained by iteratively selecting the top discriminative features as tree nodes and aggregating multiple trees with the weights determined from subset of the training samples. Thus, the tree nodes and the weights in the model reflect their impacts to the prediction, which is driven by the training data, making the model interpretable. For instance, larger values of inflammatory markers, such as LDH, ferritin, CRP drive to a positive prediction. These markers have been reported to be significantly associated with high risk of the development of COVID-19 and disease progression *(9, 22)*. Smaller values of WBC, lymphocyte count, neutrophil count, and monocyte count drive to a negative prediction. Lymphopenia, neutropenia and leukopenia are observed in a proportion of COVID-19 patients at hospital admission *(7, 23)* and are common features in severe COVID-19 patients *(3, 24)*. It is noteworthy that the control group in the training set were patients negative for COVID-19 but ill for other diseases. That may explain why smaller values of a few lab tests, such as troponin, ALK, indirect bilirubin, were seen in the SARS-CoV-2 positive group compared to the control groups.

There are three potential limitations to the use of this model. First, the model was trained on a dataset generated from a patient cohort who were in the hospital for moderate to life-threatening presentations of COVID-19. Thus, this model may not be applicable to mild COVID-19 cases. Second, the model was developed with a “control

medRxiv preprint doi: https://doi.org/10.1101/2020.06.17.20133892; this version posted June 19, 2020. The copyright holder for this preprint (which was not certified by peer review) is the author/funder, who has granted medRxiv a license to display the preprint in perpetuity. It is made available under a CC-BY-NC-ND 4.0 International license .

group" of ill patients in a metropolitan hospital for other causes. Thus, the model may need further refinement with different non-COVID population such as patients seen in a primary care office. Third, clinical application of the proposed model may require modification of laboratory testing practice to include tests that are not currently part of the institutional COVID-like illness (CLI) laboratory test panel.

Despite the robust retrospective performance of our model, prospective studies are necessary to evaluate cost-effectiveness and correlation with patient outcome in clinical practice. As many hospitals have established criteria for SARS-CoV-2 RT-PCR testing based on a variety of factors, including patient symptoms, the robustness of the supply chain as well as the skills and numbers of laboratory personnel, future studies are needed to perform a comprehensive evaluation of the proposed model on diverse patient populations including those with mild COVID-19 and those outside a large metropolitan hospital setting.

Conclusions:

We trained and tested a machine learning model incorporating 27 routine laboratory tests to provide a rapid and objective assessment of patient SARS-COV-2 infection status. The robust performance of our model was confirmed in an independent testing set. Our results have illustrated the potential role for this model as a complementary diagnostic tool to identify high-risk SARS-COV-2 infected patients before their RT-PCR results are available, and risk stratify patients in the ED. As such use of our model could result in earlier appropriate treatment and isolation, thereby promoting the health of the patients while protecting the health of the public. Furthermore, our model may play an important role in assisting in the identification of

medRxiv preprint doi: https://doi.org/10.1101/2020.06.17.20133892; this version posted June 19, 2020. The copyright holder for this preprint (which was not certified by peer review) is the author/funder, who has granted medRxiv a license to display the preprint in perpetuity. It is made available under a CC-BY-NC-ND 4.0 International license .

SARS-COV-2 infected patients in areas where RT-PCR testing is not possible due to financial or supply constraints.

medRxiv preprint doi: https://doi.org/10.1101/2020.06.17.20133892; this version posted June 19, 2020. The copyright holder for this preprint (which was not certified by peer review) is the author/funder, who has granted medRxiv a license to display the preprint in perpetuity. It is made available under a CC-BY-NC-ND 4.0 International license .

Acknowledgement:

We want to thank Richard Fedeli for organizing the datasets of laboratory testing results.

Author contribution:

HSY for conceptualization, investigation, data analysis, writing, reviewing and editing of the manuscript, and visualization. LVV for organizing LMH data; PS for editing the manuscript and providing ED information; AC for editing the manuscript; YH for performing data analysis; SER, MMC, ML, RK for editing the manuscript; ZZ for conceptualization and editing the manuscript; FW for conceptualization, investigation, data analysis, visualization, editing the manuscript, and supervision of project.

Conflict of Interests Disclosure:

None of the authors have conflict of interest in this project.

Funding/Support: The work of FW and YH is supported by National Science Foundation under grant number 1750326 and 1716432, and Office of Naval Research under grant number N00014-18-1-2585

medRxiv preprint doi: https://doi.org/10.1101/2020.06.17.20133892; this version posted June 19, 2020. The copyright holder for this preprint (which was not certified by peer review) is the author/funder, who has granted medRxiv a license to display the preprint in perpetuity. It is made available under a CC-BY-NC-ND 4.0 International license .

References:

1. Dong E, Du H, Gardner L. An interactive web-based dashboard to track covid-19 in real time. Lancet Infect Dis 2020.
2. Chavez S, Long B, Koyfman A, Liang SY. Coronavirus disease (covid-19): A primer for emergency physicians. Am J Emerg Med 2020.
3. Guan WJ, Ni ZY, Hu Y, Liang WH, Ou CQ, He JX, et al. Clinical characteristics of coronavirus disease 2019 in china. N Engl J Med 2020.
4. Sethuraman N, Jeremiah SS, Ryo A. Interpreting diagnostic tests for sars-cov-2. JAMA 2020.
5. Prevention CfDCa. Interim guidelines for collecting, handling, and testing clinical specimens for covid-19. 2020.
6. Mei X, Lee HC, Diao KY, Huang M, Lin B, Liu C, et al. Artificial intelligence-enabled rapid diagnosis of patients with covid-19. Nat Med 2020.
7. Physicians ACoE. The american college of emergency physicians guide to coronavirus disease (covid-19). 2020.
8. Lippi G, Plebani M. Laboratory abnormalities in patients with covid-2019 infection. Clin Chem Lab Med 2020.
9. Wu C, Chen X, Cai Y, Xia J, Zhou X, Xu S, et al. Risk factors associated with acute respiratory distress syndrome and death in patients with coronavirus disease 2019 pneumonia in wuhan, china. JAMA Intern Med 2020.
10. Ferrari D, Motta A, Marta S, Banfi G, Locatelli M. Routine blood tests as a potential diagnostic tool for covid-19. Clinical Chemistry Laboratory Medicine 2020.

medRxiv preprint doi: https://doi.org/10.1101/2020.06.17.20133892; this version posted June 19, 2020. The copyright holder for this preprint (which was not certified by peer review) is the author/funder, who has granted medRxiv a license to display the preprint in perpetuity. It is made available under a CC-BY-NC-ND 4.0 International license .

11. Than MP, Pickering JW, Sandoval Y, Shah ASV, Tsanas A, Apple FS, et al. Machine learning to predict the likelihood of acute myocardial infarction. Circulation 2019.

12. Tomasev N, Glorot X, Rae JW, Zielinski M, Askham H, Saraiva A, et al. A clinically applicable approach to continuous prediction of future acute kidney injury. Nature 2019;572:116-9.

13. Liang HY, Tsui BY, Ni H, Valentim CCS, Baxter SL, Liu G, et al. Evaluation and accurate diagnoses of pediatric diseases using artificial intelligence. Nature Medicine 2019;25:433-+.

14. Mei XY, Lee HC, Diao KY, Huang MQ, Lin B, Liu CY, et al. Artificial intelligence-enabled rapid diagnosis of patients with covid-19. Nature Medicine 2020.

15. Yan L, Zhang H, Goncalves J, Xiao Y, Wang M, Guo Y, Sun C, Tang X, Jing L, Zhang M, Huang X, Xiao Y, Cao H, Chen Y, Ren T, Wang F, Xiao Y, Huang S, Tan X, Huang N, Jiao B, Cheng C, Zhang Y, Luo A, Mombaerts L, Jin J, Cao Z, Li S, Xu H, Yuan Y. An interpretable mortality prediction model for covid-19 patients. Nature Machine Intelligence 2020;2:283-8.

16. Liu R, Han H, Liu F, Lv Z, Wu K, Liu Y, et al. Positive rate of rt-pcr detection of sars-cov-2 infection in 4880 cases from one hospital in wuhan, china, from jan to feb 2020. Clin Chim Acta 2020;505:172-5.

17. Breiman L, Friedman J, Stone CJ, Olshen RA. Classification and regression trees. 1 edition Ed.: Chapman and Hall/CRC; 1984.

18. Breiman L. Random forests. Machine learning 2001;45:5-32.

medRxiv preprint doi: https://doi.org/10.1101/2020.06.17.20133892; this version posted June 19, 2020. The copyright holder for this preprint (which was not certified by peer review) is the author/funder, who has granted medRxiv a license to display the preprint in perpetuity. It is made available under a CC-BY-NC-ND 4.0 International license .

19. Friedman J. Greedy function approximation: A gradient boosting machine. Annals of statistics 2001;29:1189-232.

20. Fluss R, Faraggi D, Reiser B. Estimation of the youden index and its associated cutoff point. Biom J 2005;47:458-72.

21. Lundberg SM, Lee SI. A unified approach to interpreting model predictions. Adv Neur In 2017;30.

22. Terpos E, Ntanasis-Stathopoulos I, Elalamy I, Kastritis E, Sergentanis TN, Politou M, et al. Hematological findings and complications of covid-19. Am J Hematol 2020.

23. Fan BE, Chong VCL, Chan SSW, Lim GH, Lim KGE, Tan GB, et al. Hematologic parameters in patients with covid-19 infection. Am J Hematol 2020;95:E131-E4.

24. Cao X. Covid-19: Immunopathology and its implications for therapy. Nat Rev Immunol 2020;20:269-70.

medRxiv preprint doi: https://doi.org/10.1101/2020.06.17.20133892; this version posted June 19, 2020. The copyright holder for this preprint (which was not certified by peer review) is the author/funder, who has granted medRxiv a license to display the preprint in perpetuity. It is made available under a CC-BY-NC-ND 4.0 International license .

Figure legends:

Figure 1. Illustration of the modeling pipeline. Routine laboratory testing results completed within two days prior to the release of RT-PCR results were used to construct a vector, upon which we built a classifier to predict the RT-PCR positive or negative result. Each dimension of the vector corresponds to a specific laboratory test, and its value corresponds to the average of all results of this laboratory test taken during the collection window. The model outputs a probability score ranging from 0 – 1, indicating the risk of SARS-Cov-2 infection.

Figure 2. Performance of four models using five-fold cross validation on the test set. (a) Comparison of the ROC curves for the gradient boosted decision tree (GBDT) model, random tree model, logistic regression model, and decision tree model. (b) Comparison of the AUC, sensitivity, specificity, and agreement with SARS-CoV-2 RT-PCR (at the operating point determined by the Youden Index) achieved by the four models.

Figure 3. Contribution laboratory tests to the prediction of the GBDT model, using the SHAP technique. (a) The lab tests are organized on the y-axis according to their mean absolute SHAP values shown on the x-axis, which represents how the testing results drive the prediction of the GBDT model. Individual values of each test for each patient are colored according to their relative values. (b) Representative force plot of a patient who had a negative RT-PCR result at the initial ED visit. The GBDT model predicts a positive probability score of 0.95. Lab tests in red are positive “force” whereas test in blue are negative “force” driving the COVID-19 positive prediction.

medRxiv preprint doi: https://doi.org/10.1101/2020.06.17.20133892; this version posted June 19, 2020. The copyright holder for this preprint (which was not certified by peer review) is the author/funder, who has granted medRxiv a license to display the preprint in perpetuity. It is made available under a CC-BY-NC-ND 4.0 International license .

Table 1: Summary of the statistics and p-values of 27 laboratory tests selected to construct the input feature vectors to the classification model. The demographic information used for p-value adjustment includes age, gender and race.

feature name	p-value	p-value (Bonferroni correction)	p-value (demographics adjustment)	Total Median (25% - 75% quantile)	Positive Median (25% - 75% quantile)	Negative Median (25% - 75% quantile)
Anion gap	1.15E-16	4.15E-15	9.91E-10	9.3 (8.0, 11.19)	10.0 (8.5, 12.0)	9.0 (7.5, 11.0)
Albumin	1.24E-04	4.47E-03	5.37E-04	3.1 (2.6, 3.6)	3.10 (2.65, 3.5)	3.2 (2.56, 3.7)
Alkaline phosphatase	2.09E-27	7.51E-26	4.49E-10	82.0 (63.0, 117.5)	74.5 (58.0, 102.0)	88.5 (68.0, 129.0)
Indirect bilirubin	6.01E-14	2.16E-12	3.73E-10	0.3 (0.2, 0.5)	0.3 (0.2, 0.4)	0.4 (0.25, 0.55)
BUN/Creatinine Ratio	1.20E-06	4.31E-05	2.19E-05	19.0 (14.33, 26.0)	18.5 (14.0, 24.5)	20.0 (15.0, 27.0)
Calcium	7.96E-49	2.87E-47	2.17E-40	8.7 (8.25, 9.2)	8.5 (8.1, 8.9)	8.9 (8.4, 9.4)
Chloride	1.93E-26	6.96E-25	5.66E-18	103.0 (99.5, 106.0)	102.0 (98.33, 05.0)	103.5 (100.5, 106.0)
Globulin	4.52E-36	1.63E-34	1.53E-24	3.3 (2.8, 3.7)	3.4 (3.10, 3.8)	3.1 (2.7, 3.6)
Glucose	1.07E-13	3.87E-12	6.27E-12	112.5 (96.17, 140.5)	116.0 (100.0, 148.31)	109.75 (94.0, 134.0)
Sodium	4.83E-23	1.74E-21	1.65E-13	139.0 (136.0, 141.0)	138.0 (135.0, 140.0)	139.0 (137.0, 141.33)
Total Protein	8.45E-07	3.04E-05	3.09E-07	6.5 (5.9, 7.0)	6.5 (6.0, 7.0)	6.4 (5.7, 7.0)
Basophil count	7.20E-40	2.59E-38	3.14E-26	0.4 (0.25, 0.7)	0.30 (0.2, 0.5)	0.5 (0.3, 0.75)
Hematocrit	3.77E-42	1.36E-40	4.92E-42	37.10 (31.64, 41.1)	38.7 (34.6, 42.5)	36.0 (29.6, 40.1)
Hemoglobin	1.21E-40	4.37E-39	7.44E-41	12.4 (10.4, 13.8)	13.0 (11.45, 14.2)	12.0 (9.8, 13.5)
White blood cell (WBC)	1.02E-34	3.68E-33	2.76E-04	8.1 (5.7, 11.02)	6.9 (5.0, 9.78)	8.7 (6.3, 11.7)
Lymphocyte count	2.09E-32	7.54E-31	4.94E-02	1.0 (0.7, 1.5)	0.9 (0.6, 1.25)	1.2 (0.75, 1.7)

medRxiv preprint doi: https://doi.org/10.1101/2020.06.17.20133892; this version posted June 19, 2020. The copyright holder for this preprint (which was not certified by peer review) is the author/funder, who has granted medRxiv a license to display the preprint in perpetuity. It is made available under a CC-BY-NC-ND 4.0 International license .

Mean corpuscular hemoglobin (MCH)	9.22E-07	3.32E-05	4.81E-05	30.1 (28.6, 31.5)	29.9 (28.5, 31.2)	30.2 (28.7, 31.8)
Mean corpuscular volume (MCV)	7.37E-10	2.65E-08	1.32E-07	89.9 (86.0, 93.6)	89.1 (85.5, 92.7)	90.3 (86.5, 94.1)
Monocyte count	6.88E-28	2.48E-26	6.61E-22	0.6 (0.4, 0.8)	0.5 (0.4, 0.7)	0.6 (0.5, 0.9)
Neutrophil count	1.61E-08	5.81E-07	3.43E-09	5.55 (3.6, 8.5)	5.2 (3.4, 7.8)	5.8 (3.85, 9.2)
Red blood cell count	7.00E-50	2.52E-48	3.05E-48	4.16 (3.52, 4.65)	4.4 (3.9, 4.8)	4.0 (3.3, 4.5)
Red blood cell distribution width (RDW-CV)	1.60E-19	5.76E-18	1.31E-19	14.4 (13.5, 16.1)	14.1 (13.4, 15.2)	14.7 (13.6, 16.6)
Troponin-I	2.83E-05	1.02E-03	9.34E-04	0.03 (0.03, 0.06)	0.03 (0.03, 0.05)	0.03 (0.03, 0.09)
C-reactive protein	3.53E-28	1.27E-26	1.89E-15	7.0 (2.5, 15.30)	9.9 (4.45, 17.4)	3.8 (0.6, 10.5)
Ferritin	9.15E-19	3.29E-17	2.75E-02	567.0 (222.5, 1327.2)	733.6 (331.8, 1396.1)	374.5 (105.9, 1016.5)
Lactic acid dehydrogenase (LDH)	1.82E-33	6.54E-32	8.13E-06	354.8 (257.0, 479.0)	397.0 (304.75, 517.0)	291.0 (226.0, 410.0)
Magnesium	1.58E-04	5.70E-03	8.84E-03	1.95 (1.8, 2.2)	2.0 (1.8, 2.2)	1.93 (1.8, 2.1)

medRxiv preprint doi: https://doi.org/10.1101/2020.06.17.20133892; this version posted June 19, 2020. The copyright holder for this preprint (which was not certified by peer review) is the author/funder, who has granted medRxiv a license to display the preprint in perpetuity. It is made available under a CC-BY-NC-ND 4.0 International license .

Table 2. Basic demographics of the patients based on their first RT-PCR testing result.

	WCM				LMH			
	Total (n =3,346)	Positive (n =1,394)	Negative (n =1,952)	P-value (Positive vs. Negative)	Total (n =1,456)	Positive (n = 490)	Negative (n = 966)	P-value (Positive vs. Negative)
Gender	-	-	-	2.55e-27	-	-	-	1.83e-13
Male n (%)	1,553 (46.41 %)	801 (51.58%)	752 (48.42%)	-	630 (43.27%)	278 (44.13%)	352 (55.87%)	-
Female n (%)	1,793 (53.59%)	593 (33.07%)	1,200 (66.93%)	-	826 (56.73%)	212 (25.67%)	614 (74.33%)	-
Age (SD)	56.44 (19.48)	61.43 (17.57)	52.87 (19.98)	3.09e-37	56.20 (20.83)	65.79 (18.22)	51.34 (20.39)	3.68e-36
19-40 years n (%)	900 (26.9%)	189 (21%)	711 (79%)	-	477 (32.76%)	57 (11.95%)	420 (88.05%)	-
40-60 years n (%)	886 (26.48%)	403 (45.49%)	483 (54.51%)	-	329 (22.6%)	110 (33.43%)	219 (66.57%)	-
Age >60 years n (%)	1560 (46.62%)	802 (51.41%)	758 (48.59%)	-	650 (44.64%)	323 (49.69%)	327 (50.31%)	-
Race	-	-	-	1.20E-04	-	-	-	0.48
Caucasian n (%)	1136 (33.95%)	346 (30.46%)	790 (69.54%)	-	259 (17.79%)	59 (22.78%)	200 (77.22%)	-
African American	320 (9.56%)	135 (42.19%)	185 (57.81%)	-	159 (10.92%)	41 (25.79%)	118 (74.21%)	-
Other	421 (12.58%)	221 (52.49%)	200 (47.51%)	-	143 (9.82%)	47 (32.87%)	96 (67.13%)	-
Unknown	1224 (36.58%)	622 (50.82%)	602 (49.18%)	-	655 (44.99%)	265 (40.46%)	390 (59.54%)	-

medRxiv preprint doi: https://doi.org/10.1101/2020.06.17.20133892; this version posted June 19, 2020. The copyright holder for this preprint (which was not certified by peer review) is the author/funder, who has granted medRxiv a license to display the preprint in perpetuity. It is made available under a CC-BY-NC-ND 4.0 International license .

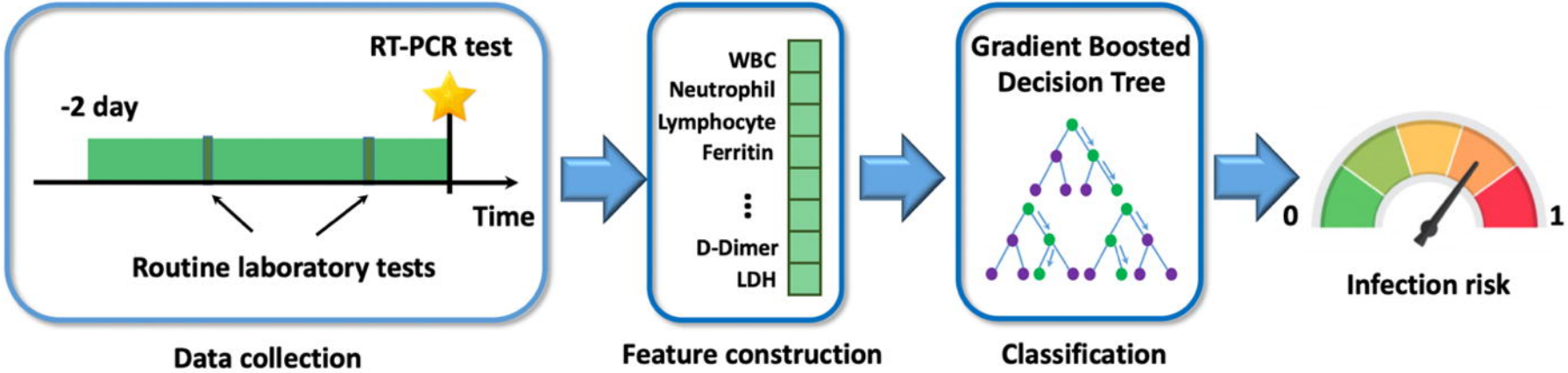
RT-PCR test
-2 day
Time
Routine laboratory tests
Data collection
WBC
Neutrophil
Lymphocyte
Ferritin
D-Dimer
LDH
Feature construction
Gradient Boosted Decision Tree
Classification
0
1
Infection risk

(a)

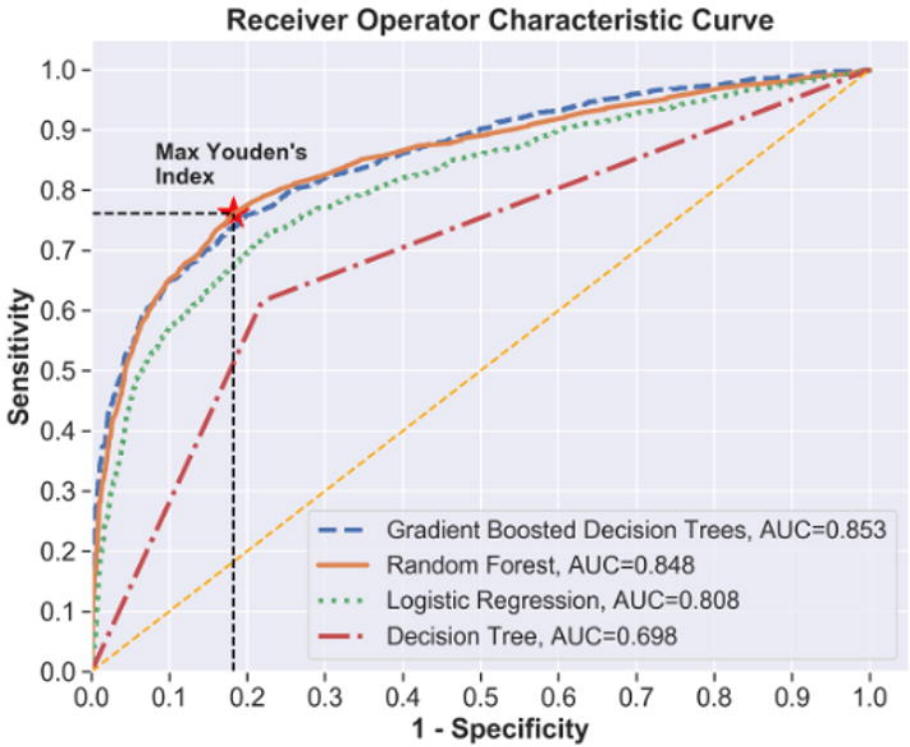

(b)

	AUC	Sensitivity	Specificity	Agreement with RT-PCR
GBDT	0.853 (0.829-0.878)	0.758 (0.662-0.812)	0.802 (0.767-0.909)	0.786 (0.772-0.828)
Random Forest	0.848 (0.823-0.874)	0.761 (0.660-0.806)	0.818 (0.777-0.906)	0.796 (0.774-0.830)
Logistic Regression	0.808 (0.781-0.836)	0.713 (0.604-0.782)	0.790 (0.725-0.886)	0.761 (0.738-0.800)
Decision Tree	0.698 (0.669-0.731)	0.610 (0.571-0.681)	0.783 (0.735-0.811)	0.718 (0.689-0.746)

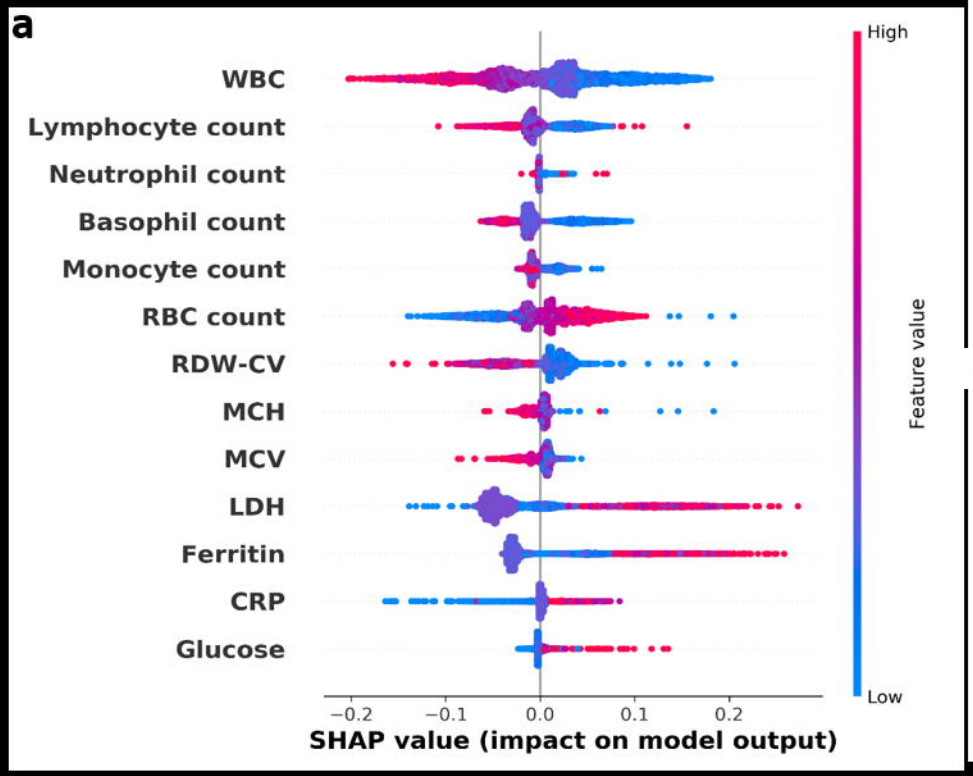
a
WBC
Lymphocyte count
Neutrophil count
Basophil count
Monocyte count
RBC count
RDW-CV
MCH
MCV
LDH
Ferritin
CRP
Glucose
−0.2
−0.1
0.0
0.1
0.2
SHAP value (impact on model output)
High
Feature value
Low

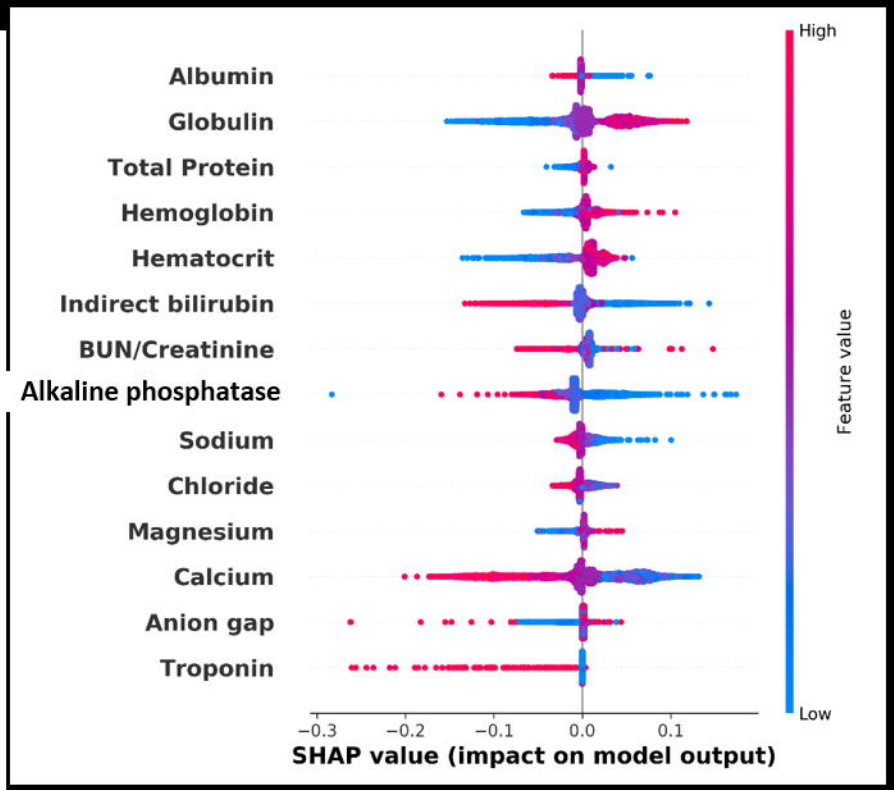
Albumin
Globulin
Total Protein
Hemoglobin
Hematocrit
Indirect bilirubin
BUN/Creatinine
Alkaline phosphatase
Sodium
Chloride
Magnesium
Calcium
Anion gap
Troponin
−0.3
−0.2
−0.1
0.0
0.1
SHAP value (impact on model output)
High
Feature value
Low

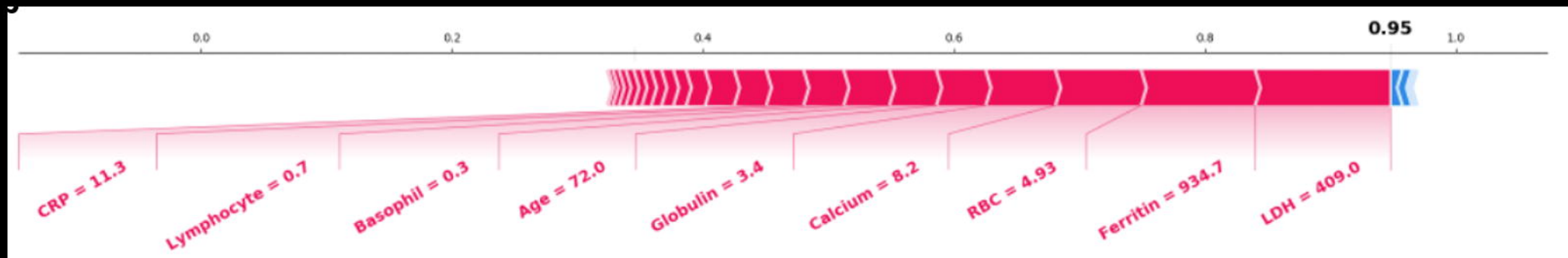
Higher
Lower
0.0
0.2
0.4
0.6
0.8
0.95
1.0
CRP = 11.3
Lymphocyte = 0.7
Basophil = 0.3
Age = 72.0
Globulin = 3.4
Calcium = 8.2
RBC = 4.93
Ferritin = 934.7
LDH = 409.0